

# Experimental Assessment of the Thermodynamic Theory of the Compositional Variation of $T_g$ : PVC Systems

J. R. FRIED and S.-Y. LAI,\* *Department of Chemical and Nuclear Engineering, Polymer Research Center, University of Cincinnati, Cincinnati, Ohio 45221*, and L. W. KLEINER and M. E. WHEELER, *Diamond Shamrock Corporation, Painesville, Ohio 44077*

## Synopsis

The glass-transition temperatures ( $T_g$ 's) and specific heats ( $C_p$ ) of poly(vinyl chloride) (PVC) and PVC plasticized with 5–120 phr di(2-ethylhexyl) adipate (DOA) and tri(2-ethylhexyl) trimellitate (TOTM) have been determined by differential scanning calorimetry (DSC). Measured  $T_g$ 's were compared to predictions by the Couchman and Karasz (C–K) thermodynamic theory, three related empirical equations, and a new equation obtained from the C–K relation by assuming the product  $T_g \Delta C_p$  to be constant. It was found that the  $T_g$ 's of the PVC/TOTM mixtures are adequately predicted only by the C–K and the derivative relation. The  $T_g$ 's of the PVC/DOA mixtures follow a sigmoidal or cusp-like dependence on plasticizer composition as has been observed for some other PVC/plasticizer mixtures. In this case, the approximation afforded by the C–K or derivative equations is still superior to the empirical models over a wide composition range. Dynamic mechanical analysis of the PVC/DOA mixtures suggests that the DSC transitions may consist of two overlapping phase transitions. The reported sigmoidal composition dependence of the DSC  $T_g$ 's may therefore result from the measured  $T_g$ 's being weighted towards the temperature corresponding to the predominant dynamic mechanical transition (i.e., the high  $T_g$  phase at low plasticizer concentrations and the low  $T_g$  phase at high plasticizer concentrations). In such cases of partial phase separation, the C–K or the derivative equation may be used to estimate the composition of the two phases at each overall plasticizer concentration.

## INTRODUCTION

Over the years, numerous equations have been used in an attempt to relate the glass-transition temperature ( $T_g$ ) of polymer mixtures to component properties.<sup>1</sup> These have been either totally empirical or derived from thermodynamic or free volume arguments; however, none of these have proved totally successful in predicting  $T_g$ 's of both polymer blends and polymer/diluent mixtures.<sup>2,3</sup> Recently, Couchman and Karasz<sup>4–6</sup> (C–K) have offered a thermodynamic derivation based on the continuity of mixture entropy at  $T_g$ . The form of the C–K equation is given as

$$\ln(T_g/T_{g,1}) = \frac{W_2 \Delta C_{p,2} \ln(T_{g,2}/T_{g,1})}{W_1 \Delta C_{p,1} + W_2 \Delta C_{p,2}} \quad (1)$$

for components 1 and 2 in a binary mixture where component 1 is the low  $T_g$  component,  $W$  is the weight fraction, and  $\Delta C_p$  is the difference in specific heat between the liquid and glass states at  $T_g$ . The utility of eq. (1) in predicting the  $T_g$ 's of miscible polymer blends was demonstrated by Couchman for two blends

\* Present address: Singer Link Division, Silver Spring, MD.

TABLE I  
 Thermal Properties

Polymer	Designation	$T_g$ (°K)	$\Delta C_p$ , (cal/g/°K)	$T_g \Delta C_p$ (cal/g)	Ref. <sup>a</sup>
Poly(2,6-dimethyl-1,4-phenylene oxide)	PPO	489	0.0528	25.8	30
Poly( $\alpha$ -methyl styrene)	PAMS	428	0.062	26.5	7
Poly(styrene-co- $\alpha$ -methyl styrene-co-acrylonitrile)	P(S-AMS-AN)	396	0.072	28.5	7
Polystyrene	PS	378	0.0671	25.4	30
Poly(vinyl chloride)	PVC	360	0.074	26.6	This study
Poly(vinyl chloride), stabilized	—	358	0.077	27.6	This study
Tricresyl phosphate	TCP	221	0.114	25.2	This study
Tri(2-ethylhexyl) trimellitate	TOTM	201	0.136	27.3	This study
Di(2-ethylhexyl) phthalate	DOP	186	0.145	27.0	This study
Di(2-ethylhexyl) adipate	DOA	173	0.154	26.6	This study

<sup>a</sup> Reference to values of both  $T_g$  and  $\Delta C_p$ .

of poly(2,6-dimethyl-1,4-phenylene oxide) (PMMPO)<sup>5</sup> and more recently by Leisz et al.<sup>7</sup> for four additional polymer blends including two PVC blends.

Couchman<sup>5</sup> showed that under certain restrictions, eq. (1) reduces to several empirical relations. For example, if  $\Delta C_{p,1} = \Delta C_{p,2}$ , eq. (1) reduces to the logarithmic rule of mixtures<sup>8</sup>

$$\ln(T_g/T_{g,1}) = W_2 \ln(T_{g,2}/T_{g,1}) \quad (2a)$$

or upon rearrangement

$$\ln T_g = W_1 \ln T_{g,1} + W_2 \ln T_{g,2} \quad (2b)$$

If the ratio of the two components  $T_g$ 's ( $T_{g,2}/T_{g,1}$ ) is not very far from unity, second- and higher-order terms in the series expansion of the logarithmic terms in eq. (2a) can be neglected to give the following equation which is known as the simple rule of mixtures

$$T_g = W_1 T_{g,1} + W_2 T_{g,2} \quad (3)$$

It is evident that if the C-K relation is valid and if the  $T_g$ 's of the mixture's two components are widely separated as they are for polymer/diluent mixtures, then the linear relation of eq. (3) would be a poor approximation to actual mixture  $T_g$ 's. This also should be true for eq. (2) which was obtained on the assumption that  $\Delta C_p$  is constant. As Boyer and Simha<sup>9,10</sup> have shown, it is the product of  $T_g \Delta C_p$ , rather than  $\Delta C_p$  alone, which is approximately constant for amorphous glasses. The assumption of constant  $\Delta C_p$  on which derivation of eq. (2) depends therefore also implies the limiting restriction that  $T_{g,2} \approx T_{g,1}$ . Boyer<sup>10</sup> has reported that for 30 different polymers, the product  $T_g \Delta C_p$  was found to be 27.5 cal/g. We have determined values of  $T_g \Delta C_p$  for six polymers and four amorphous low-molecular-weight plasticizers (Table I) and found that  $T_g \Delta C_p \approx 26.1$  cal/g in good agreement with Boyer's value. As shown in Table I for a variety of amorphous glasses whose  $T_g$ 's range from 489 to 173°K,  $\Delta C_p$  is not constant but varies between 0.0528 to 0.154 cal/g/°K.

As published  $T_g$  data rarely include values of component  $\Delta C_p$ , it is difficult to assess the validity of eq. (1) for other mixtures, particularly polymer/diluent systems for which  $T_g$  varies widely with composition. Under such circumstances,

TABLE II  
P(S-AN-AMS)/PVC<sup>a</sup>

$W_1$	$\Delta C_p$ (cal/g/°K)	Glass transition temperature (°K)					
		expt.	eq. (1)	eq. (4)	eq. (5)	eq. (2)	eq. (3)
0	0.072	396	—	—	—	—	—
0.2	—	387	386.8	386.2	386.6	387.0	387.4
0.4	—	378	377.9	377.0	377.6	378.2	378.8
0.6	—	369	369.3	368.5	369.0	369.6	370.2
0.8	—	362	361.0	360.5	360.8	361.2	361.6
1.0	0.074	353	—	—	—	—	—

<sup>a</sup> Reference 7.

a useful form of the C-K relation is obtained by allowing the product  $T_g \Delta C_p$  in eq. (1) to be a constant. Upon rearrangement, eq. (1) then becomes

$$\ln(T_g/T_{g,1}) = \frac{W_2 \ln(T_{g,2}/T_{g,1})}{W_1(T_{g,2}/T_{g,1}) + W_2} \quad (4)$$

In the limiting case where  $T_{g,1} \approx T_{g,2}$ , truncation of the expansion of the logarithmic terms leads to a limiting form of eq. (4) which is the inverse rule of mixtures or Fox equation<sup>11</sup>

$$1/T_g = W_1/T_{g,1} + W_2/T_{g,2} \quad (5)$$

which also may be obtained through an expansion of the logarithmic terms of eq. (2a).

Tables II-IV show comparison between literature values of  $T_g$ 's and those calculated by use of eqs. (1)-(5) for three PVC systems. As indicated for the case of a blend of PVC with a miscible terpolymer of styrene, acrylonitrile, and  $\alpha$ -methylstyrene (Table II), all five equations give good predictions of actual

TABLE III  
PVC/DCHP<sup>a</sup>

$W_1$	$\Delta C_p$ (cal/g/°K)	Glass transition temperature (°K)					
		expt.	eq. (1)	eq. (4)	eq. (5)	eq. (2)	eq. (3)
0	—	350	—	—	—	—	—
0.009	—	348	—	348.1	348.4	348.7	348.4
0.018	—	346	—	346.2	346.9	347.4	347.9
0.039	—	342	—	341.9	343.9	344.5	345.4
0.058	—	337	—	338.1	340.1	341.8	343.2
0.107	—	329	—	328.9	332.2	335.1	337.5
0.209	—	315	—	311.8	316.8	321.5	325.5
0.306	—	303	—	307.6	303.4	309.0	314.2
0.405	—	292	—	284.9	290.9	296.8	302.6
0.408	—	284	—	284.6	290.5	296.5	302.3
0.455	—	277	—	279.1	284.9	290.8	296.8
0.503	—	268	—	273.8	279.4	285.2	291.1
0.556	—	262	—	268.3	273.9	279.1	284.9
0.608	—	256	—	263.3	268.1	273.3	278.9
0.652	—	252	—	259.2	263.7	268.4	273.7
0.706	—	248	—	254.5	258.4	262.6	267.4
1.0	—	233	—	—	—	—	—

<sup>a</sup> Reference 12.

TABLE IV  
PVC/DOP<sup>a</sup>

$W_1$	$\Delta C_p$ (cal/g/°K)	Glass transition temperatures (°K)					
		expt.	eq. (1)	eq. (4)	eq. (5)	eq. (2)	eq. (3)
0	0.077 <sup>b</sup>	368	—	—	—	—	—
0.20	—	303	294.3	291.3	306.1	320.0	331.0
0.30	—	270	269.4	266.3	282.4	298.4	312.5
0.40	—	239	249.4	246.6	262.0	278.3	294.0
0.50	—	222	233.2	230.8	244.4	259.5	275.5
1.0	0.145 <sup>b</sup>	183	—	—	—	—	—

<sup>a</sup> Reference 13.<sup>b</sup> Values were obtained in the present study.

blend  $T_g$ . This is a consequence of the relatively small difference between component  $T_g$ 's,  $T_{g,2}/T_{g,1} = 1.122$  satisfying the condition for which eqs. (3)–(5) are valid approximations.

In the case of two PVC/plasticizer systems for which values of  $\Delta C_p$  were not reported, predicted values of mixture  $T_g$  by use of eqs. (2)–(5) vary widely. Comparisons of experimental and predicted  $T_g$ 's for PVC/di(cyclohexyl) phthalate (DCHP),<sup>12</sup> and PVC/di(2-ethylhexyl) phthalate (DOP),<sup>13</sup> are given in Tables III and IV and illustrated in Figures 1 and 2, respectively. These show that as the ratio of  $T_{g,2}/T_{g,1}$  increases from 1.50 for PVC/DCHP to 2.01 for PVC/DOP, eqs. (5), (2), and (3) predict increasingly higher values of  $T_g$  compared to the experimental results; however, agreement between eq. (4) values and measured  $T_g$ 's is satisfactory. In both systems, the measured  $T_g$ 's [although approximated by eq. (4)] appear to follow a nonmonotonic dependence on plasticizer composition ( $W_1$ ). Pezzin et al.<sup>12</sup> suggest that the cusp-like character of the PVC/DCHP  $T_g$ -composition curve represented by the broken line curve is due to elimination of WLF free volume by the plasticizer below 0.4 weight fraction DCHP. This cusp-like behavior has been predicted theoretically by Kovacs<sup>14</sup> on the basis of Kelly–Bueche<sup>15</sup> free volume theory. A similar composition dependence is evident for PVC/DOP in Figure 2.

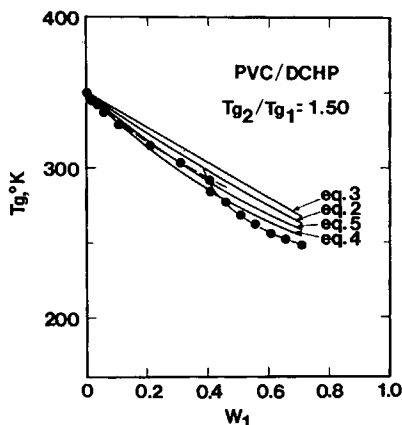


Fig. 1. Glass-transition temperatures ( $T_g$ ) of PVC/DCHP mixtures as a function of weight fraction DCHP ( $W_1$ ); data taken from Pezzin et al.<sup>12</sup>

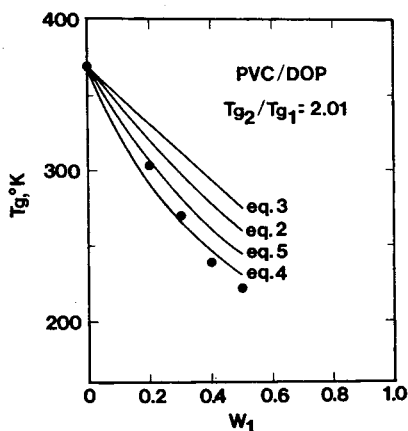


Fig. 2. Glass-transition temperatures ( $T_g$ ) of PVC/DOP mixtures as a function of weight fraction DOP ( $W_1$ ); data taken from Ref. 13.

It is the purpose of this study to compare the predictions of eqs. (1)–(5) with experimental data for two other plasticized PVC systems for which sample preparation and measurement techniques are precisely controlled. The two plasticizers chosen are di(2-ethylhexyl) adipate (DOA) and tri(2-ethylhexyl) trimellitate (TOTM) whose thermal properties are given in Table I. Comparison is made between predicted and actual  $T_g$ 's as measured by differential scanning calorimetry (DSC) and conclusions concerning system miscibility are obtained from dynamic mechanical spectra analysis.

## EXPERIMENTAL

### Materials

PVC resin was supplied by Diamond Shamrock Corporation and was specified to have a  $K$  value of 70 (0.5 g/100 ml cyclohexanone at 25°C) and typical plasticizer absorption characteristics (internal pore volume of 0.270 cm<sup>3</sup>/g). The resin had a polydispersity index ( $\bar{M}_w/\bar{M}_n$ ) of 2.5 as determined in tetrahydrofuran by gel permeation chromatography (Waters GPC/ALC 301). Plasticizers used in this study were di(2-ethylhexyl) adipate (DOA) and tri(2-ethylhexyl) trimellitate (TOTM) manufactured by Monsanto Company and Eastman Kodak, respectively. During dry blending, 3.5 phr liquid Ba/Cd/Zn stabilizer (Mark 2109, Argus Chemical Corp.) and 0.5 phr stearic acid lubricant were added.

### Sample Preparation

The PVC resin was mixed with stabilizer, lubricant, and 0–120 phr plasticizer in a Hobart mill for 5 min at room temperature. Each sample was then transferred to a 340°F (171°C) two-roll mill and melt blended for another 5 min after which time the milled sheets were cut to appropriate size and compression molded in a steam heated press for 8 min using a four-step pressure cycle (first 2 min, contact; second 2 min, 700 psi; third 2 min, 1400 psi; and final 2 min, 2100 psi). At the end of the heat cycle, the samples were slow cooled from 340°F to ambient temperature in the press at 2100 psi. Total cooling time was 13 min.

Films prepared by this procedure were clear, free of voids, and ca. 0.010 in. (0.254 mm) thick.

### Measurements

DSC thermograms were obtained at 40°C/min (Perkin-Elmer DSC II) using samples weighing 10–25 mg for molded films and 10–16 mg for liquids (plasticizers and temperature standards) at a range of 10 mc/sec. Sample weights were determined to a precision of 0.1 mg by means of a Perkin-Elmer Autobalance (AM-2). Samples were conditioned in the DSC as follows: heating from 140 to 420°K under a helium purge; equilibrium at 400–420°K for 2 min; cooling to 140°K at 160°K/min; and reheating at 40°K/min.

Following the DSC measurement, the thermograms (second heating) were converted to specific heat-temperature plots by standard sapphire calibration procedures as detailed by O'Neill.<sup>16</sup> Temperatures were calibrated by reference to transition temperatures of standard samples of indium (429.78°K), high purity *n*-octadecane (302.4°K), and *n*-heptane (182.6°K). Indium was purchased as a DSC standard from Perkin-Elmer Corp.; *n*-octadecane and *n*-heptane from the Humphrey Chemical Co. (lot Nos. 3200579 and 7040579, respectively). The glass-transition temperature ( $T_g$ ) of each sample was determined as the temperature at the midpoint ( $1/2 \Delta C_p$ ) of the transition as described by Fried et al.<sup>17</sup>

Dynamic mechanical spectra of molded films (ca. 20–25 mm in length and 2.5–5.5 mm in width) were obtained at 11 Hz using a Rheovibron DDV-II operating in the tensile mode. Values of dynamic storage ( $E'$ ) moduli, loss ( $E''$ ) moduli, and  $\tan \delta$  ( $E''/E'$ ) were determined at intervals of 5°C over a temperature range from –140°C to sample  $T_g$ . In the cases of the unplasticized PVC resin and two TOTM samples (5 and 10 phr), values of  $E'$  and  $E''$  were corrected for system compliance, sample yielding within the tensile grips, and system inertia by the method of Massa.<sup>18,19</sup> Dynamic moduli determined at three different film lengths were used in the correction procedure.

### RESULTS

Sapphire-calibrated DSC thermograms for PVC/TOTM and PVC/DOA are given in Figures 3 and 4, respectively. As illustrated by Figure 5, the thermal transition from the glass to liquid state occurs over a wide temperature range with the transition being broadest at 40 phr for both PVC/TOTM and PVC/DOA.

Glass-transition temperatures are plotted as a function of weight fraction plasticizer for PVC/TOTM and PVC/DOA in Figures 6 and 7, respectively. As shown in Figure 6 and by values given in Table V, best agreement with measured  $T_g$ 's over the largest part of the composition range of PVC/TOTM is obtained by use of eqs. (1) and (4) which give nearly identical values as a result of the near equivalency of component  $T_g \Delta C_p$ . Above 10 phr TOTM, eqs. (5), (2), and (3) predict increasingly higher values of  $T_g$  compared to measured values, while at 5 and 10 phr, eq. (5) (Fox equation) gives better fit to experimental points than eq. (4).

It is noted that although the agreement with the C-K theory is satisfactory

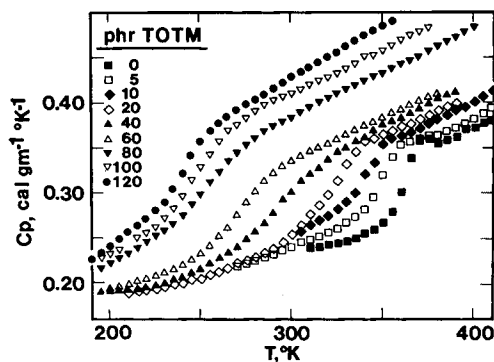


Fig. 3. Specific heat ( $C_p$ ) of PVC/TOTM mixtures as a function of temperature.

for PVC/TOTM, the experimental results at low TOTM compositions are suggestive of the cusp-like behavior exhibited by PVC/DCHP as was shown in Figure 1. This anomalous behavior is even more pronounced for PVC/DOA as illustrated in Figure 7. As indicated by  $T_g$  values given in Table VI, both eqs. (1) and (4) predict the same values of  $T_g$  within approximately  $1^\circ\text{K}$  as would be

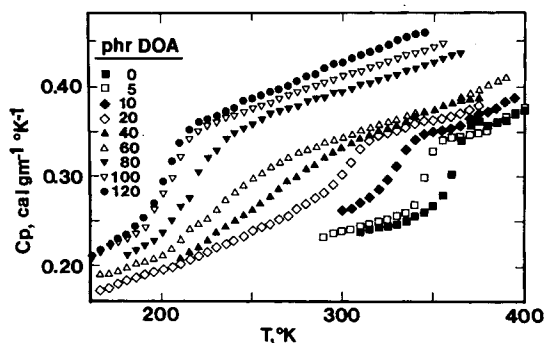


Fig. 4. Specific heat ( $C_p$ ) of PVC/DOA mixtures as a function of temperature.

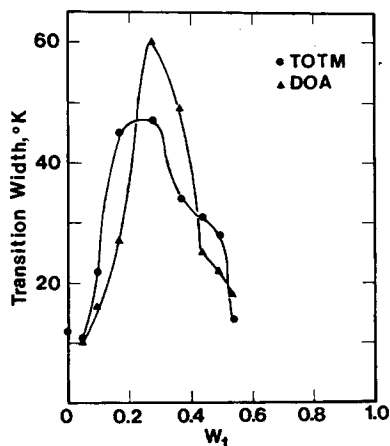


Fig. 5. Transition width at  $T_g$  as defined by Fried et al.<sup>17</sup> plotted as a function of weight fraction plasticizer ( $W_1$ ).

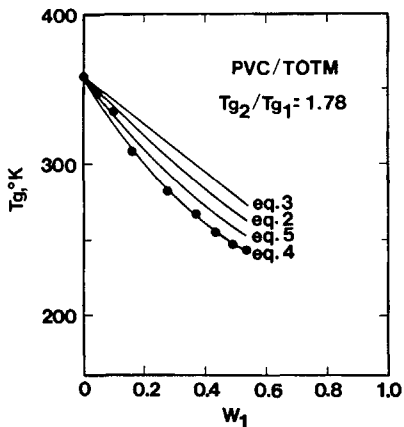


Fig. 6. Glass-transition temperatures ( $T_g$ ) of PVC/TOTM as a function of weight fraction TOTM ( $W_1$ ).

expected by the nearly equivalent values of  $\Delta C_p T_g$  for both components (Table I). As for PVC/TOTM, best agreement at low concentrations (5–20 phr) is found by use of eq. (5) (Fox equation). At higher concentrations, eq. (4) [or eq. (1)] overestimates  $T_g$  but overall provides a more satisfactory fit than either eqs. (5), (2), or (3) which significantly overestimate  $T_g$  compared to experimental values for PVC/TOTM. The inadequacy of eqs. (5), (2), and (3) compared to eq. (2) is expected because of the large  $T_{g,2}/T_{g,1}$  value (2.07 compared to 1.78 for PVC/TOTM) which invalidates the expansion approximation by which eqs. (5), (2), and (3) are obtained from eq. (1).

The effect of low concentrations of TOTM on the dynamic mechanical spectra of PVC at 11 Hz is illustrated in Figure 8. For PVC without plasticizer, a well-defined  $\beta$  transition appears at 235°K (–38°C) with a maximum in the  $\alpha$  transition ( $T_g$ ) above ca. 359°K in agreement with other studies.<sup>20–24</sup> For our slowly cooled samples, we found no evidence for a transition at ca. 300°K recently reported<sup>23</sup> for quenched PVC films. With increasing TOTM concentration, the  $\beta$  transition reduces in intensity beginning from the high-temperature side as

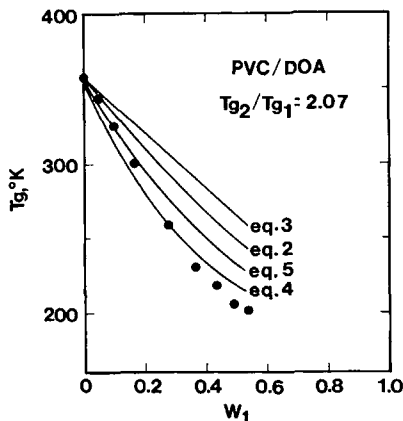


Fig. 7. Glass-transition temperatures of PVC/DOA as a function of weight fraction DOA ( $W_1$ ).



TABLE V  
PVC/TOTM

phr TOTM	$W_1$	$\Delta C_p$ (cal/g/°K)	Glass transition temperature (°K)					
			expt.	eq. (1)	eq. (4)	eq. (5)	eq. (2)	eq. (3)
0	0	0.077	358	—	—	—	—	—
5	0.046	—	347	342.1	342.0	345.6	348.6	350.8
10	0.096	—	334	326.8	326.6	333.0	338.7	342.9
20	0.161	—	308	309.3	309.0	318.0	326.2	332.7
40	0.278	—	382	283.4	283.1	294.1	304.9	314.4
60	0.366	—	267	267.2	267.2	278.4	289.8	300.5
80	0.435	—	255	256.7	256.4	267.2	278.5	289.7
100	0.490	—	247	249.0	248.7	258.9	269.8	281.1
120	0.536	—	243	242.1	242.8	252.3	262.7	273.8
—	1.0	0.136	201	—	—	—	—	—

observed for other PVC/plasticizer systems;<sup>20,22</sup> however, there is evidence of multiple transitions within the  $\beta$  relaxation of the 5 and 10 phr TOTM samples. There appears to be a low-temperature peak at ca. 210°K and a high-temperature transition at ca. 270°K at 5 phr TOTM. The high-temperature transition is shifted downward to ca. 238°K at 10 phr TOTM. These may correspond to the  $\beta_1$  relaxation at 273°K and a  $\beta_2$  relaxation at 223°K reported by Kakutani and Asahina<sup>25</sup> and speculated to result from molecular motions in the crystalline and amorphous regions, respectively

As also shown in Figure 8,  $E'$  increases with increasing plasticizer concentration at temperatures above the high-temperature side of the  $\beta$  transition as a result of the suppression of  $\beta$  relaxation and gradual elimination of the corresponding small step decrease in  $E'$  for pure PVC. This behavior is one manifestation of the antiplasticization effect widely reported for PVC/diluent systems.<sup>20,21,26-29</sup>

Comparison of the dynamic mechanical  $\tan\delta$  spectra for PVC/TOTM and PVC/DOA is given over the composition range between 5–120 phr in Figures 9–16. At 5 and 10 phr (Figs. 9 and 10, respectively) the low-temperature side of the  $\alpha$  transition of both the PVC/TOTM and PVC/DOA samples appears steep while the  $\beta$  transition of the PVC/TOTM sample is more strongly suppressed compared to PVC/DOA. At 20 phr (Fig. 11) the  $\alpha$  transition appears to rise more gradually and a minor transition appears at about 223°K for the PVC/DOA

TABLE VI  
PVC/DOA

phr DOA	$W_1$	$\Delta C_p$ (cal/g/°K)	Glass transition temperatures (°K)					
			expt.	eq. (1)	eq. (4)	eq. (5)	eq. (2)	eq. (3)
0	0	0.077	358	—	—	—	—	—
5	0.046	—	344	335.8	335.1	341.2	346.2	349.5
10	0.096	—	326	315.2	314.0	324.7	333.9	340.2
20	0.161	—	301	292.6	291.1	305.4	318.4	328.2
40	0.278	—	259	260.9	259.3	276.0	292.5	306.6
60	0.366	—	231	242.5	241.0	257.3	274.3	290.3
80	0.435	—	219	230.4	229.0	244.3	260.9	277.5
100	0.490	—	206	221.9	220.7	234.9	250.7	267.4
120	0.536	—	202	215.5	214.4	227.6	242.4	258.8
—	1.0	0.154	173	—	—	—	—	—

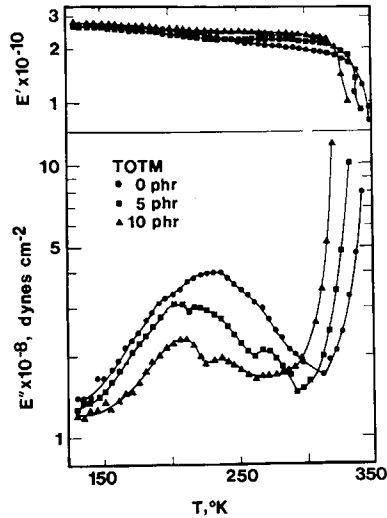


Fig. 8. Massa<sup>18,19</sup> corrected values of dynamic storage ( $E'$ ) and loss ( $E''$ ) moduli as a function of temperature for PVC and 5 and 10 phr TOTM films.

sample. At 40 phr (and higher) DOA concentration (Fig. 12), this transition increases in intensity and decreases slightly in temperature until at 80 phr (Fig. 14), it is the dominant transition and becomes merged with the high-temperature transition. By comparison, the  $\alpha$  relaxation for the PVC/TOTM samples is sharper and occurs at higher temperatures. There is evidence only for a small low-temperature shoulder at 40 phr and higher TOTM concentrations.

At all compositions and for both systems there is an appearance of a beginning of a small transition below  $150^{\circ}\text{K}$ . Similar observations have been made for other PVC/plasticizer systems by Kinjo and Nakagawa<sup>20</sup> who attributed this relaxation to molecular motions of alkyl chains of the plasticizer. For DOA and

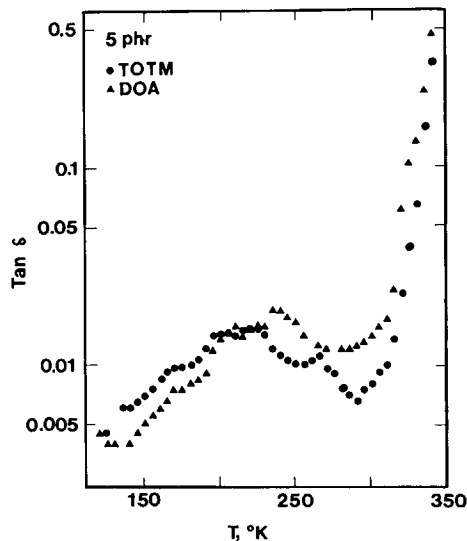


Fig. 9. Dynamic mechanical  $\tan \delta$  ( $E''/E'$ ) as a function of temperature for 5 phr TOTM and DOA films.

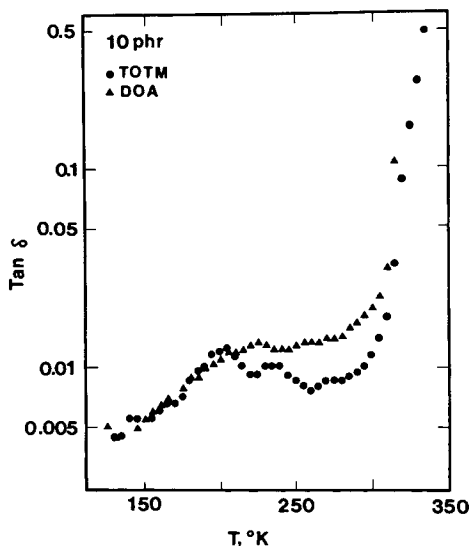


Fig. 10. Dynamic mechanical  $\tan\delta$  for 10 phr TOTM and DOA films.

TOTM, this sub- $T_g$  transition may be due to local motions of the 2-ethylhexyl substituent groups.

## DISCUSSION

There is a suggestion of slight curvature of the  $C_p$  plots of both PVC/TOTM and PVC/DOA (Figs. 3 and 4) above  $T_g$  and at low plasticizer concentration. Although we feel the present data may be inconclusive in this regard, it is noted that Bair and Warren<sup>31</sup> recently have observed a distinct second amorphous transition occurring about 20°C above the  $T_g$  of PVC for other PVC/plasticizer blends at low plasticizer (<25 wt%) content. This high-temperature transition

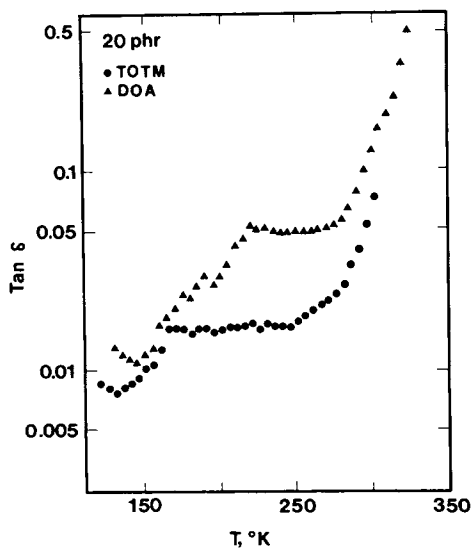


Fig. 11. Dynamic mechanical  $\tan\delta$  for 20 phr TOTM and DOA films.

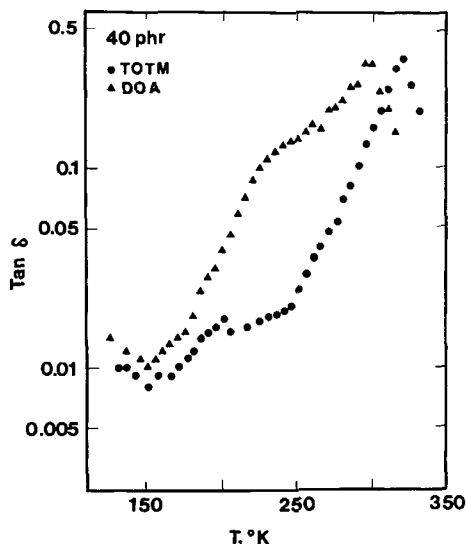


Fig. 12. Dynamic mechanical  $\tan\delta$  for 40 phr TOTM and DOA films.

was associated with microdomains (100–200 Å) of syndiotactic sequences of PVC molecules. Direct evidence for a related nodular structure in PVC has been reported by Gezovich and Geil.<sup>32</sup> Bair and Warren have suggested that at low plasticizer concentration, these domains (characterized by a high  $T_g$  due to their syndiotactic character) become swollen but not completely dissociated by plasticizer molecules. As a result, their  $T_g$  decreases at a slower rate than observed for the more highly plasticized amorphous regions. As no sequence distribution data for the PVC sample used in the present study is available, comment cannot be made on the weakness of the high  $T_g$  second amorphous transition (if any) for the PVC/TOTM and PVC/DOA blends compared to those systems studied by Bair and Warren.

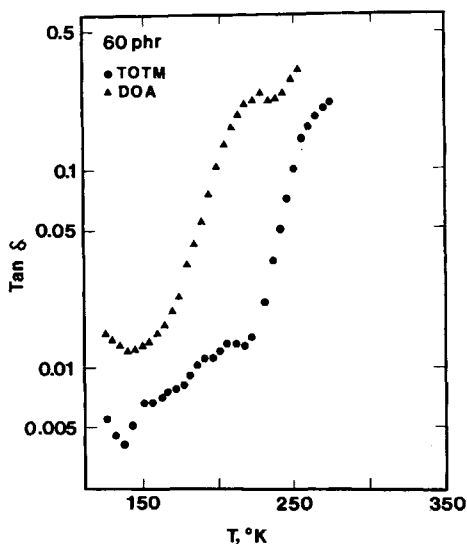


Fig. 13. Dynamic mechanical  $\tan\delta$  for 60 phr TOTM and DOA films.

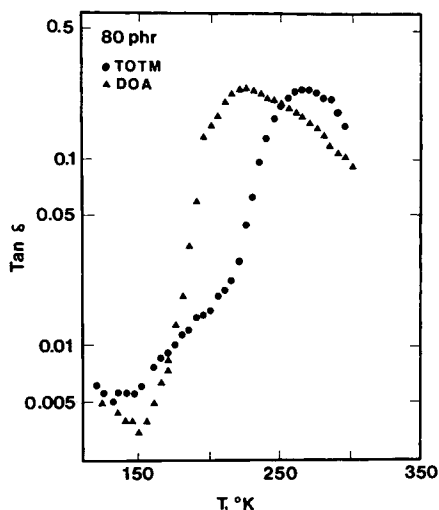


Fig. 14. Dynamic mechanical  $\tan\delta$  for 80 phr TOTM and DOA films.

The dynamic mechanical spectra appearing in Figures 9–16 clearly indicate the presence of two coexisting phases in the PVC/DOA mixtures; a high  $T_g$  (PVC-rich) phase and a low  $T_g$  (DOA-rich) phase. For example, at 40 phr DOA (Fig. 12) the transition corresponding to the DOA-rich phase appears as a pronounced shoulder on the low-temperature side of the main  $\alpha$  transition with a maximum intensity estimated at 263°K. At 60 phr (Fig. 13) this DOA-rich phase transition appears to be shifted to 233°K. By comparison, the PVC-rich phase transition of the PVC/TOTM mixtures is relatively sharp and well separated from a minor phase transition occurring at 208°K for 60 phr TOTM (Fig. 13). At 80–120 phr (Figs. 14–16), the DOA-rich (low  $T_g$ ) transition is the predominant transition while the corresponding transition for the PVC/TOTM mixtures is a minor shoulder centered at 193°K. The low-temperature location, small in-

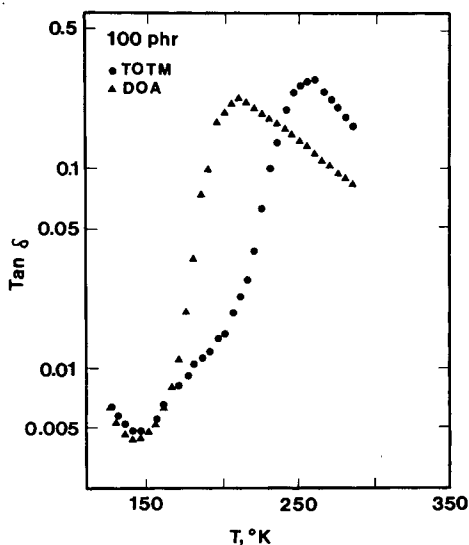


Fig. 15. Dynamic mechanical  $\tan\delta$  for 100 phr TOTM and DOA films.

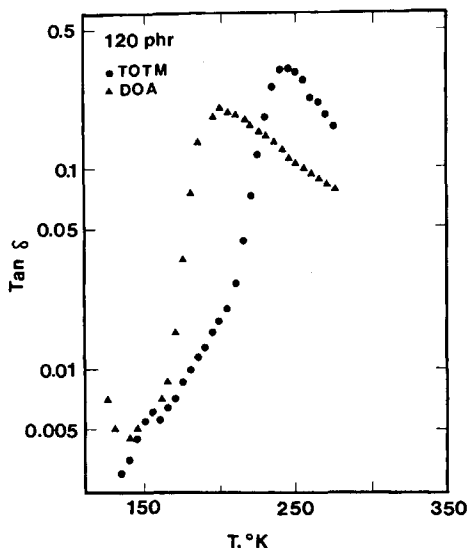


Fig. 16. Dynamic mechanical  $\tan\delta$  for 120 phr TOTM and DOA films.

tensity, and relative compositional invariance of this minor transition for PVC/TOTM suggests that it may correspond to the  $\alpha$  relaxation of a small amount of pure TOTM (DSC  $T_g$  of 201°K) not dispersed in the PVC resin.

The conclusion reached by these results is that TOTM forms a more homogeneous mixture with PVC than does DOA under the conditions by which these samples were prepared. The good agreement between measured  $T_g$ 's and those predicted by the C-K equation for PVC/TOTM mixtures above 10 phr supports this conclusion. This is also suggested by a comparison of the solubility parameter (Hoy) of PVC (9.54) with those for DOA (8.08) and TOTM (8.62) which suggests a higher thermodynamic miscibility of PVC/TOTM ( $\delta_2 - \delta_1 = 0.92$ ) compared to PVC/DOA ( $\delta_2 - \delta_1 = 1.46$ ).

The anomalous  $T_g$ -composition dependence indicated by the DSC results for PVC/DOA may be explained in the following manner. At low DOA concentrations (up to 20 phr DOA), the PVC-rich (high- $T_g$ ) transition is dominant and as a result the DSC transition reflects a high  $T_g$  compared to the C-K prediction. At high DOA concentrations (80-120 phr), the low  $T_g$  transition in the dynamic mechanical spectra is the dominant transition resulting in a low  $T_g$  measured by DSC. The consequence of these effects may be the observed sigmoidal  $T_g$ -composition curve illustrated in Figure 7. It is possible that such reasoning may be used to explain the similar composition dependence of  $T_g$  observed for PVC/DOP (Fig. 1) and PVC/DCHP (Fig. 2). Further study of these systems appears warranted. The reason for the slightly high value of  $T_g$  observed for PVC/TOTM at 5 and 10 phr (Fig. 6) is not immediately clear although there is a suggestion of the beginning of a high-temperature shoulder in the Massa corrected  $E'$  plots at these concentrations (Fig. 8).

One of us (J.R.F.) acknowledges partial research support for this study from the Research Council of the University of Cincinnati. We also wish to thank Mr. Thomas Reed of Diamond Shamrock Corporation for his invaluable assistance in sample preparation and Dr. Edward A. Collins for his interest in encouraging this work.

## References

1. J. R. Fried, in *Developments in Polymer Characterization-4*, J. V. Dawkins, Ed., Applied Science, London, to appear.
2. M. C. Shen and A. V. Tobolsky, *Adv. Chem. Ser.*, **48**, 27 (1965).
3. A. Packer and M. S. Neerurkar, *Kolloid Z. Polym.*, **229**, 7 (1969).
4. P. R. Couchman and F. E. Karasz, *Macromolecules*, **11**, 117 (1978).
5. P. R. Couchman, *Macromolecules*, **11**, 1156 (1978).
6. P. R. Couchman, SPE National Conference Papers, Boston, May 4-7, 1981, pp. 849-850.
7. D. M. Leisz, L. W. Kleiner, and P. G. Gertenbach, *Thermochim. Acta*, **35**, 51 (1980).
8. J. M. Pochan, C. L. Beatty, and D. F. Pochan, *Polymer*, **20**, 879 (1979).
9. R. Simha and R. F. Boyer, *J. Chem. Phys.*, **37**(5), 1003 (1962).
10. R. F. Boyer, *J. Macromol. Sci. Phys.*, **B7**(3), 487 (1973).
11. T. G. Fox, *Bull. Am. Phys.*, **1**, 123 (1956).
12. G. Pezzin, A. Omacini, and F. Zilio-Grandi, *Chim. Ind. (Milan)*, **50**, (3) 309 (1968).
13. W. P. Brennan, Thermal Analysis Application Study 11, Perkin-Elmer Corp., Order No. TAAS-11.
14. A. J. Kovacs, *Fortschr. Hochpolym. Forsch.*, **3**(3), 394 (1964).
15. F. N. Kelley and F. Beuche, *J. Polym. Sci.*, **50**, 549 (1961).
16. M. J. O'Neill, *Anal. Chem.*, **38**, 1331 (1966).
17. J. R. Fried, F. E. Karasz, and W. J. MacKnight, *Macromolecules*, **11**, 150 (1978).
18. D. J. Massa, J. R. Flick, and S. E. B. Petrie, *Am. Chem. Soc., Div. Org. Coat. Plast. Chem. Pap.*, **35**(1), 371 (1975).
19. D. J. Massa, *J. Appl. Phys.*, **44**(6), 2595 (1973).
20. N. Kinjo and T. Nakagawa, *Polym. J.*, **4**(2), 143 (1970).
21. H. Bertilsson and J. F. Jansson, *J. Macromol. Sci. Phys.*, **B14**(2), 251 (1977).
22. G. Pezzin, G. Ajroldi, and C. Garbuglio, *J. Appl. Polym. Sci.*, **11**, 2553 (1967).
23. R. Diaz Calleja, *Polym. Eng. Sci.*, **19**(8), 596 (1976).
24. L. M. Robeson, *Polym. Eng. Sci.*, **9**(4), 277 (1969).
25. H. Kakutani and M. Asahina, *J. Polym. Sci., Polym. Phys. Ed.*, **7**, 1473 (1969).
26. R. A. Horsley, in *Progress in Plastics 1957*, P. Morgan, Ed., Hiffe and Sons, London, 1957, pp. 77-88.
27. R. B. Seymour and C. W. Greenup, *Plast. Aust.*, **22**(9), 15 (1971).
28. N. Kinjo, *Jpn. Plast.*, **7**(4), 6, 28 (1973).
29. K. Nakamura, F. Hashimoto, M. Nakanishi, N. Kinjo, T. Komatsu, and T. Nakagawa, *Proc. 5th Int. Congr. Rheol.*, **3**, 409 (1976).
30. J. R. Fried, Ph.D. Dissertation, University of Massachusetts (Amherst), 1976; Xerox University Microfilms, Ann Arbor, 77-6467.
31. H. E. Bair and P. C. Warren, *J. Macromol. Sci. Phys.*, **B20**, 381 (1981).
32. D. M. Gezovich and P. H. Geil, *Int. J. Polym. Mater.*, **1**, 3 (1971).

Received November 3, 1981

Accepted January 18, 1982